

Structural, Optical, Elemental and Thermal Characteristics of Pure and Magnesium Sulfate-Doped Growth Thiourea Crystals

D. Priya Dharshini^a, C. Hentry^b and B. Leema Rose^b

^a Research Scholar (Reg.no: 19213232132011), Department of Physics, St. Jude's College, Thoothoor, Affiliated to Manonmaniam Sundaranar University, Abishekapatti, Tirunelveli, 627012, Tamilnadu, India.

^b Department of Physics, St. Jude's College, Thoothoor, 629176, Tamilnadu, India.

Doi:

Received on: 06/03/2023;

Accepted on: 18/07/2023

Abstract: The growth of single crystals of pure and magnesium sulfate (MgSO₄)-doped Thiourea (TU) was accomplished by solvent evaporation. The grown crystals were characterised by X-ray powder diffraction, FTIR, EDAX, UV-visible, and TG/DTA techniques. The MgSO₄-doped TU crystal has good optical transmission in the entire visible range. The metal complexes of TU enhanced the lower cut-off wavelength by 14.85 nm compared to pure TU, which is an essential requirement for a nonlinear optical material.

Keywords: Optical material, Magnesium sulphate, Gravimetric, Structural resemblance, Thiourea.

1. Introduction

Low-temperature solution growth is the simplest and, in many cases, the least expensive method for the production of optical crystals. Nonlinear optical materials (NLO) have a number of applications, such as second harmonic generation, frequency mixing, electro optic modulation, etc. Organic NLO materials are attracting investigators for possible use in optical devices because of their large optical nonlinearity, low cut-off wavelength, short response time, and high laser damage threshold

[1]. TU is the class of organic compounds having sulphur with the general formula (R₁R₂N)(R₃R₄N)C=S. These have a structural resemblance to urea, except that the oxygen atom of urea is replaced by a sulphur atom. The chemical properties of urea and TU are quite different from each other [2]. TU derivatives are used in drug design and medicinal chemistry. Fig. 1 (a) and (b) represent the chemical structures of TU and urea, respectively.

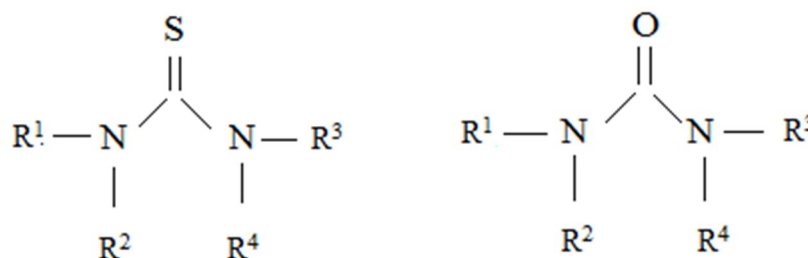


FIG. 1. (a) Thiourea and (b) Urea.

TU is an interesting inorganic matrix modifier, and it has the ability to form an extensive network of hydrogen bonds [3]. TU inorganic metal complex crystals with interesting optical, crystalline perfection, dielectric, mechanical, and electronic properties, as evidenced by investigators, are bis(TU) cadmium chloride, bis(TU) zinc chloride, bis(TU) cadmium acetate, bis(TU) cadmium acetate [4, 5], etc. The molecular structure of TU has been investigated using C2 symmetry constraints [6]. Organic ligands and small-electron systems such as TU, thiocyanate, and urea have been used with remarkable success. The Centro symmetric TU molecule, when combined with an inorganic salt, yields non-Centro symmetric complexes, which have NLO properties [7]. TU crystals also exhibit a pyro electric effect, which is utilised in infrared (IR), ultraviolet (UV), scanning electron microscopy (SEM), and infrared imaging [8]. TU is one of the few simple organic compounds with high crystallographic symmetry. It crystallises in the rhombic pyramidal division of the rhombic system and acts as a good ligand [9]. TU forms a

number of NLO-active metal coordination compounds [10-14].

In the present investigation, pure and various mole percentages of $MgSO_4$ of doped TU have been grown by solvent evaporation technique.

2. Experimental

2.1. Materials

All the reagents used in the present study were of analytical grade. Thiourea (99%) was purchased from Merck. The solvent used in all the experiments was double-distilled water.

2.2. Temperature Dependence on Solubility

The maximum amount of solute that dissolves in a known quantity of solvent at a certain temperature is its solubility. Temperature will affect solubility. In the present investigation, the solubility of TU and $MgSO_4$ -doped TU in double-distilled water was estimated at various temperatures ranging from 25°C to 50°C in steps of 5°C by the gravimetric method and presented in Table 1.

TABLE 1. Solubility of TU and $MgSO_4$ -doped TU in double-distilled water.

Temperature (°C)	Solubility pure TU g/L	Solubility $MgSO_4$ doped TU
25	141.5	145.4
30	163.9	167.1
35	190.5	194.4
40	234.5	238.2
45	280.2	284.1
50	414.9	418.3

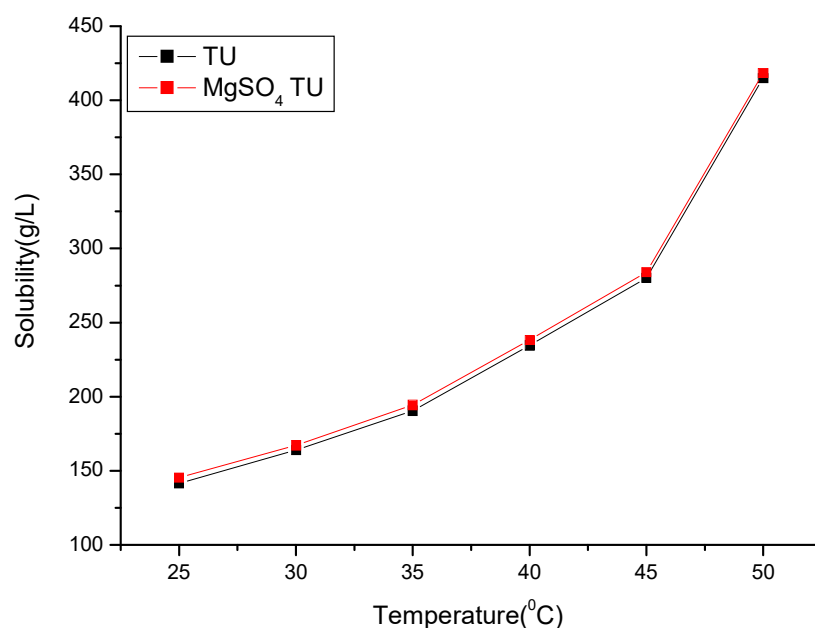


FIG. 2. Solubility curve of TU and $MgSO_4$ doped TU.

The collected data shows that the solubility of TU increases with an increase in temperature; the addition of MgSO_4 to the pure TU solution increased the solubility and had a positive temperature coefficient of solubility.

2.3. Crystal growth

350 ml of saturated solution of TU was dissolved in double-distilled water using a magnetic stirrer at a constant rate for 6 hours at a temperature of 30°C . After attaining saturation, the solution was filtered using Whatman filter paper of porous size 11.5mm. A clean and dry 250-ml beaker was used in the present investigation. 50 ml of the saturated solution was taken from seven such bakers. One beaker was

left as standard for pure TU solution. In all the other beakers, the solution was doped with 0.1 M%, 0.2 M%, 0.3 M%, 0.4 M%, 0.5 M%, and 0.6 M% of magnesium sulphate. All the crystallizers were covered with perforated polythene paper and kept on a vibration-free platform. After a period of 21 days, fully matured, pure, and MgSO_4 -doped TU could be grown. Fig. 3 (a) shows the crystal of pure TU; (b), (c) and (d) show the MgSO_4 lightly doped TU crystals; (e), (f) and (g) show the heavily doped MgSO_4 TU crystals. The morphology of the TU crystals changed as the concentration of the dopant increased.

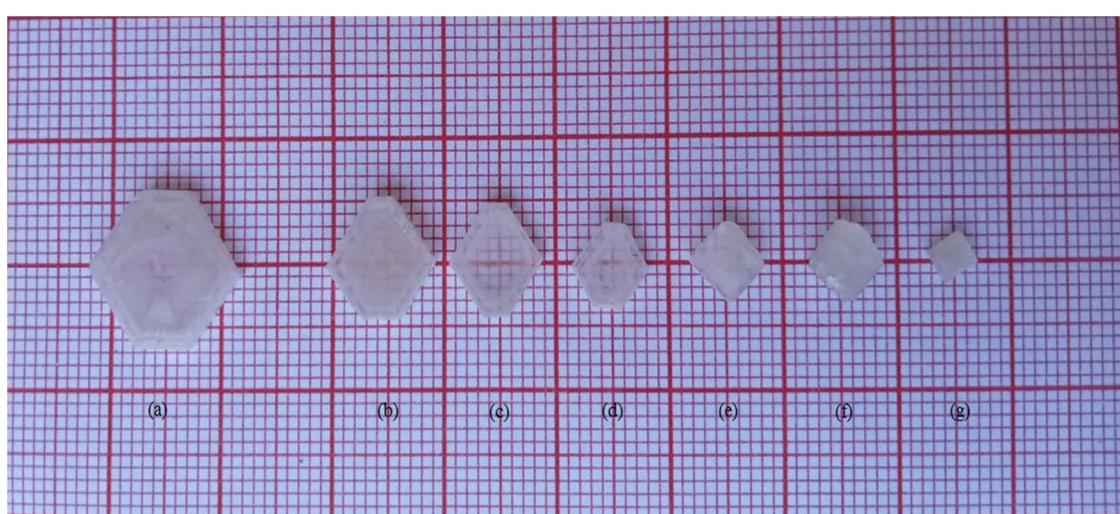


FIG. 3. Crystal habit of (a) TU; (b), (c) and (d) MgSO_4 doped TU; (e), (f) and (g) Metal complex of TU.

2.4. Characterization

The structural analysis is represented by the details from the X-ray diffractometer (P-Analytical X-Pert-Pro-Diffractometer system with $\text{CuK}\alpha$ ($K\alpha = 1.54060 \text{ \AA}$) radiation 2θ range at $10^\circ - 90^\circ$). The optical studies are performed using Fourier transform infrared spectroscopy (FTIR-Perkin Elmer wavelength range of 4500 cm^{-1} to 500 cm^{-1}). Micro morphological studies of energy dispersive x-ray analysis (EDXA, BRUKER). UV-Visible spectrophotometer (Perkin Elmer Lambda-35 UV-Vis range at 200-800 nm). Thermal analysis studies are carried

out using thermal gravimetric and differential thermal analysis (TG/DTA, NETZSCH STA 2500 at a heating rate of $20^\circ\text{C}/\text{min}$ in the temperature range of 30°C to 500°C).

3. Results and Discussion

3.1. Structural Analysis

The powder XRD patterns of pure TU, MgSO_4 -doped TU, and metal complexes of MgSO_4 -doped TU crystals are shown in Fig. 4. (a), (b) and (c), respectively.

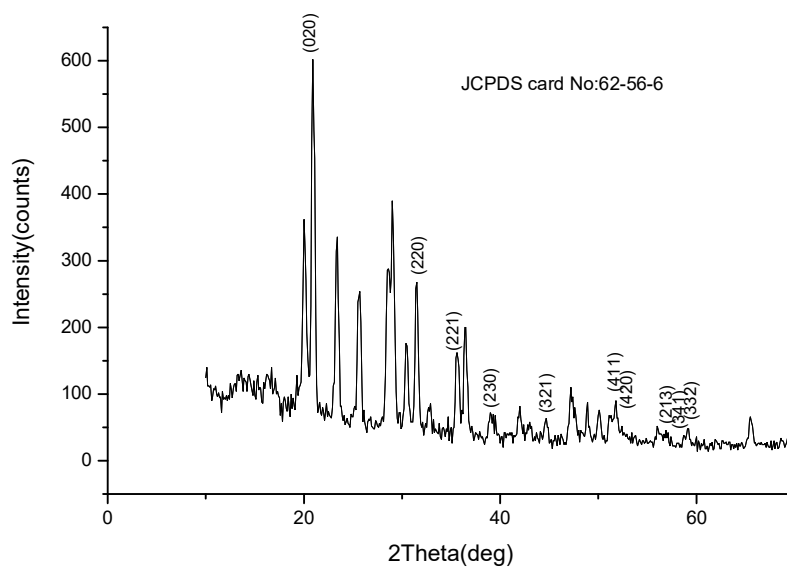


FIG. 4. (a) XRD spectrum of pure TU.

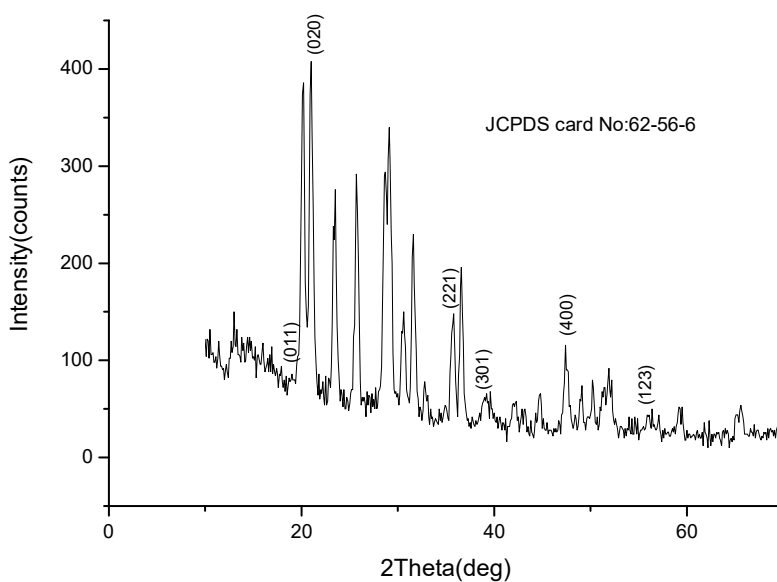
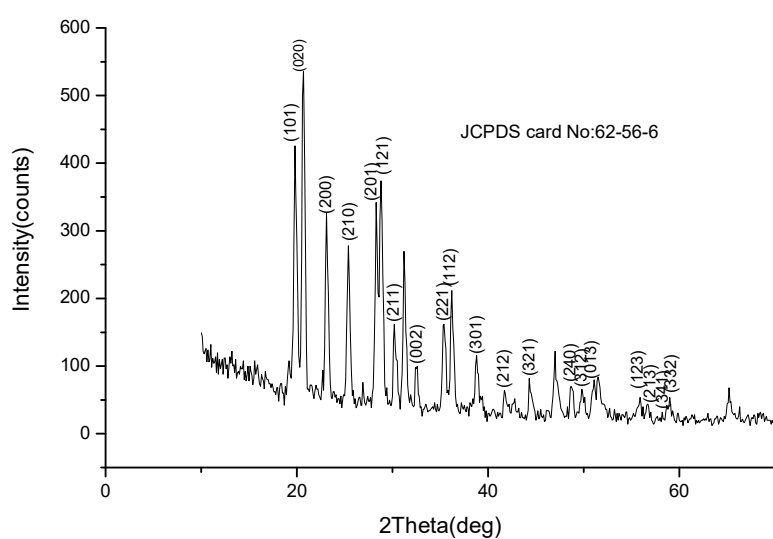
FIG. 4. (b) XRD spectrum of MgSO₄ doped TU.FIG. 4. (c) XRD spectrum of Metal complexes of MgSO₄ doped TU.

TABLE 2. Cell parameters of MgSO_4 doped TU and its metal complex.

Cell parameters (Å°)	JCPDS value of TU (Å°)	Reference value of TU (Å°) [15]	Calculated value of TU (Å°)	MgSO_4 doped TU (Å°)	Metal complexes of TU (Å°)
a	7.664	7.644	7.646	7.661	7.677
b	8.559	8.527	8.564	8.415	8.539
c	5.492	5.493	5.474	5.512	5.498
Cell volume (Å ³)	360.31	358.04	358.45	355.32	360.41

The powder XRD pattern reveals an orthorhombic crystal system. The space group of the pure and MgSO_4 -doped TU crystals was Pnma 62. Fig. 4 (a) shows the sharp peaks of pure crystal, revealing the crystallinity of grown crystals. The peak observed in the powder XRD pattern was indexed properly. The cell parameters are calculated, and the results of the cell software and the results of the cell parameters were $a = 7.646^\circ\text{Å}$, $b = 8.564^\circ\text{Å}$ and $c = 5.474^\circ\text{Å}$. The calculated cell volume of the pure crystal is 358.45°Å^3 .

Fig. 4 (b) shows the sharp peaks of MgSO_4 -doped TU crystals that reveal the crystallinity of grown crystals. The cell parameters were calculated for the observed XRD pattern by using unit cell software, and the results of the cell software and the results of the cell parameters was $a = 7.661^\circ\text{Å}$, $b = 8.415^\circ\text{Å}$ and $c = 5.512^\circ\text{Å}$. The calculated cell volume of the crystal is 355.32°Å^3 .

Fig. 4 (c) shows the sharp peaks of metal complex MgSO_4 -doped TU crystals that reveal the crystallinity of grown crystals. The cell parameters were calculated for the observed XRD pattern by using unit cell software, and the results of the cell software and the results of the cell parameters were $a = 7.677^\circ\text{Å}$, $b = 8.539^\circ\text{Å}$ and $c = 5.498^\circ\text{Å}$. The calculated cell volume of the crystal is 360.41°Å^3 .

The observed XRD pattern well matched standard JCPDS card No: 62-56-6 and the reported value, and we found a small change in the unit cell parameters in the MgSO_4 -doped TU crystals. The change in unit cell parameters of the MgSO_4 -doped crystals may be due to the presence of magnesium ions in the crystal lattice.

3.2. Vibrational Analysis

The FTIR spectra of pure TU, MgSO_4 -doped TU, and metal complexes of TU are presented in Fig. 5 (a), (b) and (c), respectively.

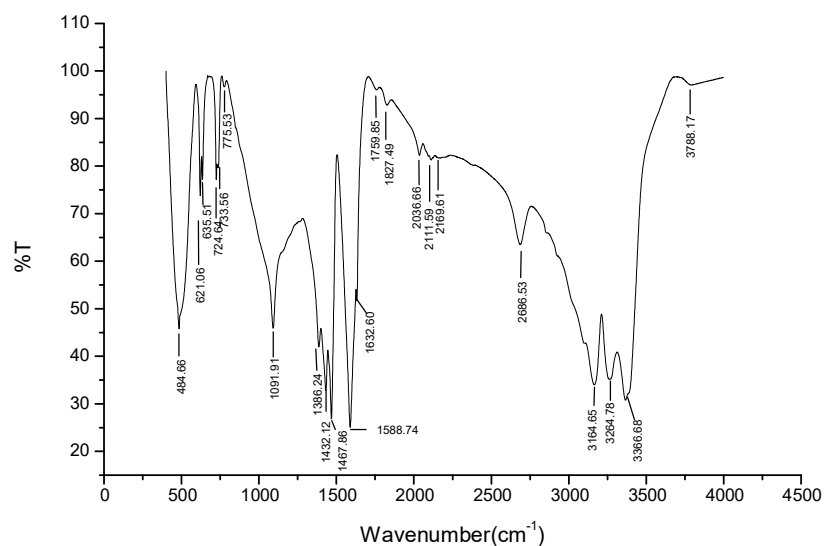
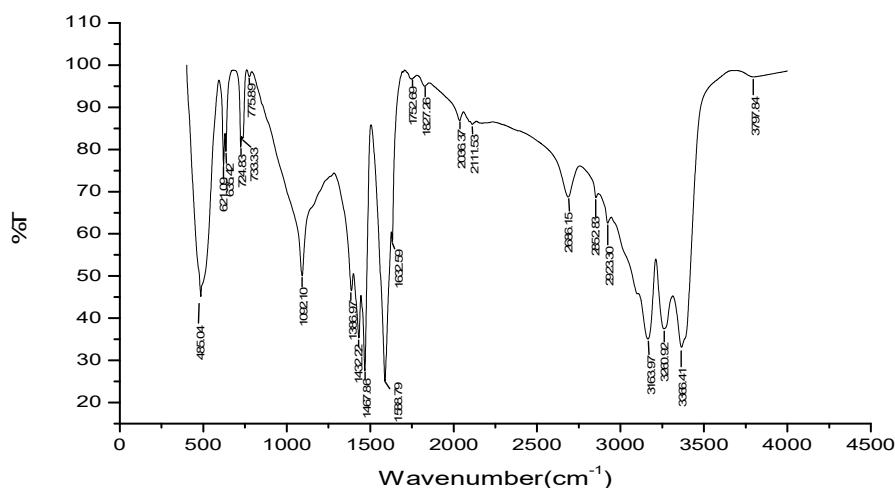
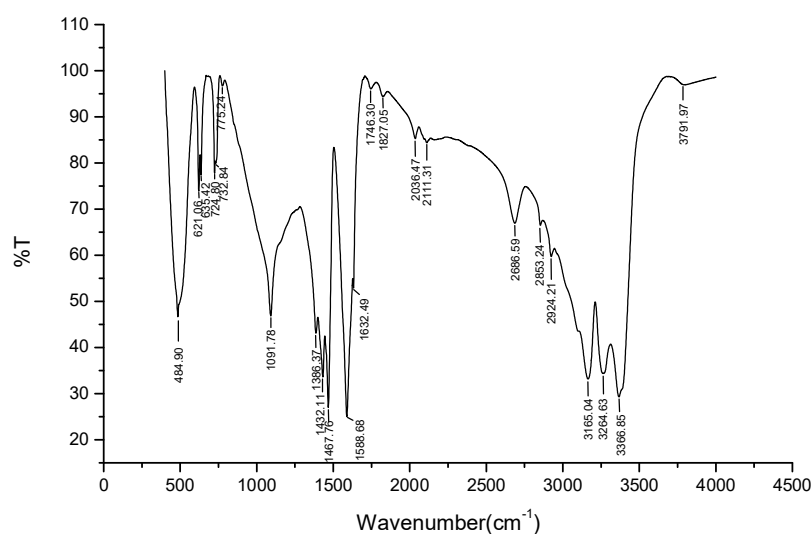


FIG. 5. (a) FTIR spectrum of pure TU.

FIG. 5. (b) FTIR spectrum of $MgSO_4$ doped TU.FIG. 5. (c) FTIR spectrum of metal complex of $MgSO_4$ doped TU.TABLE 3. Wave number assignments for pure and $MgSO_4$ -doped TU and the metal complex of $MgSO_4$ -doped TU in cm^{-1} .

Pure TU	$MgSO_4$ doped TU	Metal complex of $MgSO_4$ doped TU	Spectral Assignment
484.66	485.04	484.90	C-N-C Bending
621.06	621.09	621.06	S-O Stretching
635.51	635.42	635.42	SO_4 Bends
724.67	724.84	724.80	CH_2 Rocking vibration
733.56 and 775.53	733.56 and 775.53	732.80 and 775.24	Aromatic out of plane C-H Stretching
1091.91	1092.10	1091.78	C-O-C Asymmetric Stretching
1386.24	1386.97	1386.37	C=S Asymmetric Stretching
1432.12	1432.22	1432.11	C-N Stretching
1467.86	1467.86	1467.76	C=S Stretching
1588.74	1588.79	1588.68	N-S Scissoring
1632.60	1632.59	1632.49	N-H Bending
1759.85 and 1827.49	1752.69 and 1827.26	1746.30 and 1827.05	Symmetric C=O Stretching
2036.66	2036.66	2036.47	CH_2 rocking
2111.59	2111.59	2111.31	C \equiv C Stretching
2169.61	-	-	C \equiv C Stretching
2300-3500	2300-3500	2300-3500	NH & CH Stretching vibration
3788.17	3788.17	3791.97	O-H and C-H Stretching

The FTIR spectra of the grown pure and MgSO_4 -doped TU crystals are represented in Fig. 5 (a), (b) and (c). The spectra of the pure TU are assigned to the C-N-C bending characteristic form present at peak 484.66 cm^{-1} [16], S-O stretching characteristic form present at peak 621.06 cm^{-1} , SO_4 bending characteristic form present at peak 635.51 cm^{-1} , CH_2 Rocking vibration characteristic form present at peak 724.67 cm^{-1} , Aromatic out of plane The characteristic C-H stretching form is present at peaks of 733.56 cm^{-1} and 775.53 cm^{-1} , C-O-C Asymmetric stretching characteristic form present at peak 1091.91 cm^{-1} , C=S Asymmetric Stretching characteristics are present at peak 1386.24 cm^{-1} [17]. C-N stretching characteristic form is present at peak 1432.12 cm^{-1} , C=S Stretching characteristic form is present at peak 1467.86 cm^{-1} , N-S scissoring characteristic form is present at peak 1588.74 cm^{-1} , N-H Bending characteristic form is present at peak 1632.60 cm^{-1} . Symmetric C=O stretching characteristic form is present at peaks 1759.85 cm^{-1} and 1827.49 cm^{-1} , and CH_2 rocking characteristic form is present at peaks 2036 cm^{-1} [18]. $\text{C}\equiv\text{C}$ stretching characteristic form is present at peak 2111.59 cm^{-1} , C=C stretching characteristic form is present at peak 2169.61 cm^{-1} , NH and CH stretching characteristic forms are present at peak $2300\text{--}3500 \text{ cm}^{-1}$, O-H and C-H stretching characteristic forms are present at peak 3788.17 cm^{-1} [19]. And C=C stretching characteristic forms present at peak 2169.61 cm^{-1} [20] are absent from the MgSO_4 -doped TU and the metal complex-grown crystals. The FTIR spectral assignments of pure and MgSO_4 -doped TU and its metal complexes are shown in Fig. 5 (a), (b) and (c). So the pure TU is incorporated with the MgSO_4 -doped TU and its metal complex to form a grown crystal.

3.3. EDAX Analysis

The energy dispersive x-ray (EDAX) analysis is used to identify the elements of the grown pure and MgSO_4 -doped TU and its metal complex crystals and also find the elemental atomic weight percentage of the grown pure and MgSO_4 -doped TU and its metal complex crystals. The element analysis revealed that the elements are carbon, nitrogen, sulphur, magnesium, copper, potassium, iron, and sodium, which confirms that the samples are pure and MgSO_4 -doped TU and its metal complex. On comparing the elemental data of

pure and MgSO_4 -doped TU and its metal complex-grown crystal, copper, potassium, iron, and sodium are the only ones we found in the metal complex of MgSO_4 -doped TU. And the element magnesium is present in the MgSO_4 -doped TU and its metal complex-grown crystals. The magnesium element's atomic weight and weight percentages are higher in MgSO_4 -doped TU than its metal complex. The elements of carbon and nitrogen have increased atomic weights and weight percentages in the MgSO_4 -doped TU. And atomic weight percentages and weight percentages are decreased in the metal complex of MgSO_4 -doped TU crystals. The elemental sulphur atomic weight and weight percentages are decreased in the MgSO_4 -doped TU. And atomic weights and weight percentages are increased in the metal complex of MgSO_4 -doped TU crystals. This may be attributed to the incorporation of MgSO_4 -doped TU and its metal complex. Normally, this analysis does not acknowledge the hydrogen element. So that was the reason pure and MgSO_4 -doped TU and its metal complex element of hydrogen are not presented in the EDAX data of pure and MgSO_4 -doped TU and its metal complex crystal in Table 4. and Fig. 6 (a), (b) and (c) also.

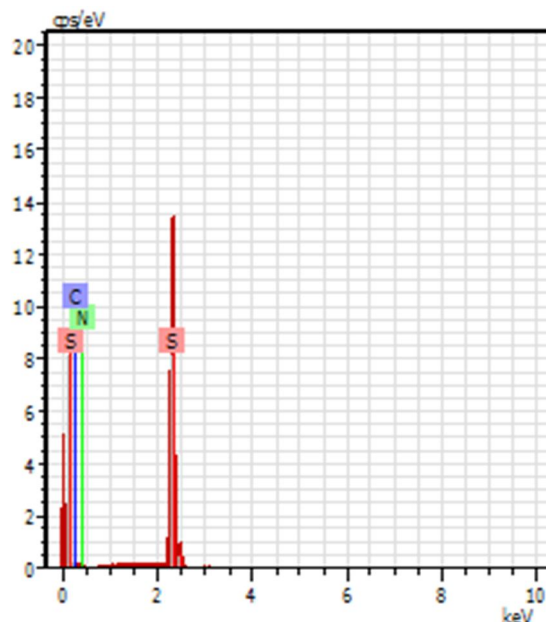


Figure 6. (a) EDAX spectrum of pure TU crystal

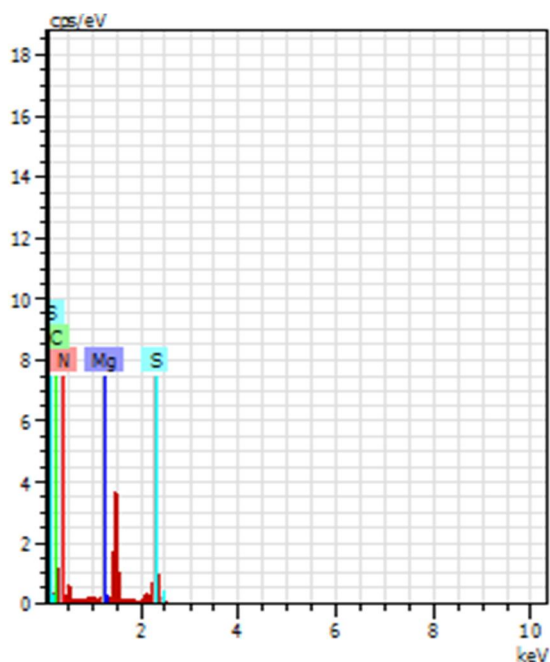


FIG. 6. (b) EDAX spectrum of MgSO_4 doped TU crystals.

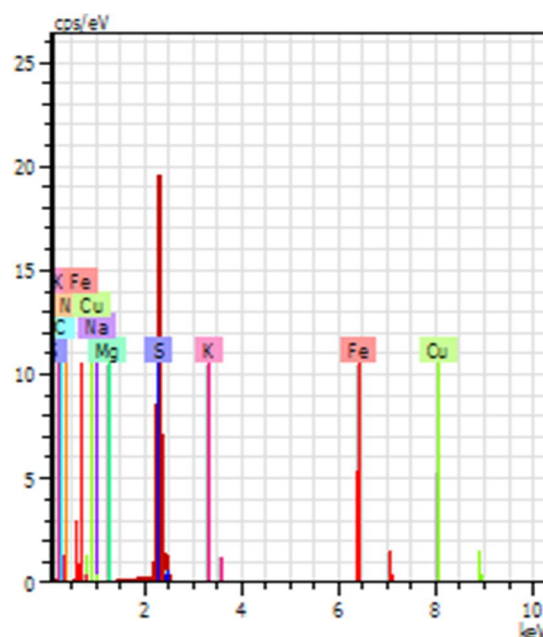


FIG. 6. (c) EDAX spectrum of Metal complexes of MgSO_4 doped TU crystals.

TABLE 4. EDAX data of pure and MgSO_4 doped TU and its metal complexes.

Elements	Pure TU		MgSO_4 doped TU		Metal complex of MgSO_4 doped TU	
	At.Wt. %	Weight%	At.Wt. %	Weight%	At.Wt. %	Weight%
C	31.21	18.89	36.80	31.61	18.26	9.08
N	33.02	23.31	58.85	58.94	23.97	13.89
S	35.77	57.80	3.39	7.78	57.41	76.18
Mg	-	-	0.96	1.67	0.03	0.03
Cu	-	-	-	-	0.28	0.72
K	-	-	-	-	0.03	0.05
Fe	-	-	-	-	0.02	0.05
Na	-	-	-	-	0.00	0.00

Table 4 shows that in pure TU crystals, only the present elements, such as carbon, nitrogen, and sulphur, were found. But in the MgSO_4 -doped TU, in addition to the parent elements, the magnesium element was highly incorporated in the parent element. However, in the metal complex of MgSO_4 -doped TU, traces of elements like potassium and iron were found.

3.4. Optical studies

An optical transmission spectrum was recorded using MgSO_4 -doped TU and its metal complex crystal range of 200 to 1200 nm using a Perkin Elmer Lambda 35 UV-Visible spectrometer to know the stability for optical

applications. From the spectra in Fig. 7. (a), (b) and (c). It was observed that the pure and MgSO_4 -doped TU and its metal complex crystals showed good transmittance in the entire visible region. The UV cut-off wavelength of pure TU crystal is found to be 376.45 nm, and there is no considerable transmission until 1200 nm. The MgSO_4 -doped TU and its metal-complex crystals are found to be 391.30 nm; both are equal, and there is no considerable transmission till 1200 nm [21]. The overlay UV-Vis spectra clearly show the optical quality of grown, pure, and MgSO_4 -doped TU and its metal complex crystals.

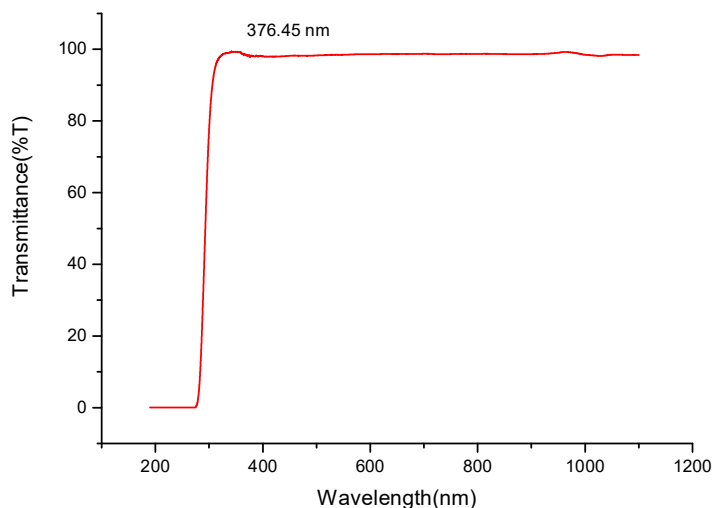


FIG. 7. (a) UV transmittance spectrum of pure TU crystal.

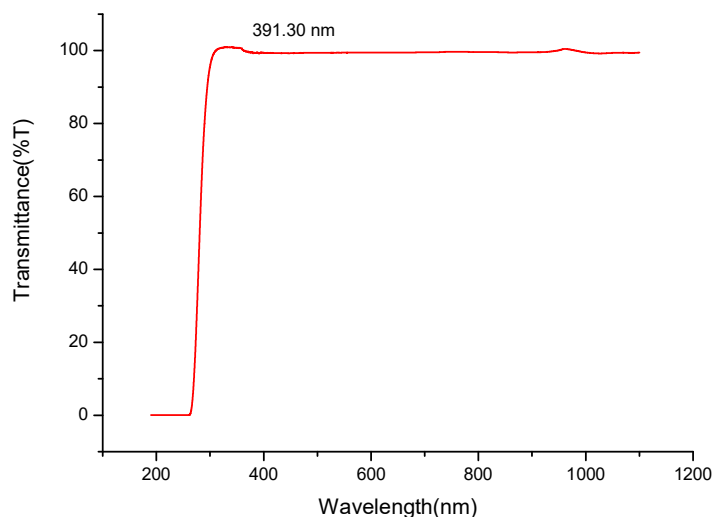


FIG. 7. (b) UV transmittance spectrum of MgSO₄ doped TU crystals

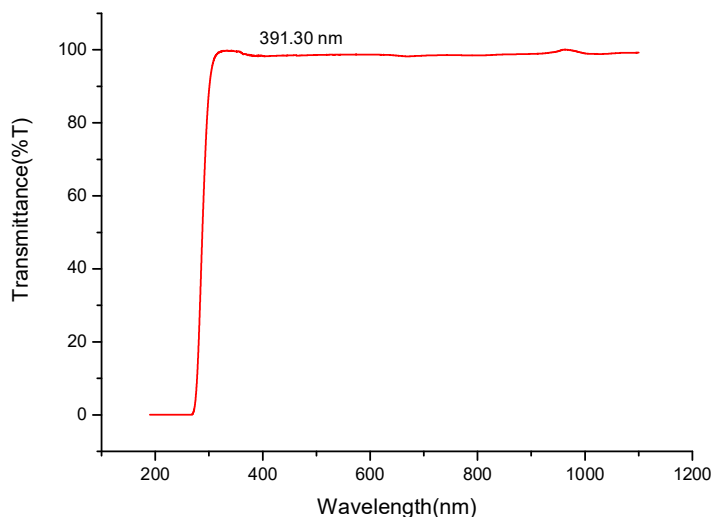


FIG. 7. (c) UV transmittance spectrum of metal complex in MgSO₄ doped TU crystals.

An optical study shows that the lower cut-off wavelength is 376.45 nm for pure TU crystals. But the lower cut-off wavelength of the doped

TU crystal was found to be enhanced by 14.85 nm, which is 14.85 nm larger than the pure TU.

3.5. Thermal Analysis

Thermo gravimetric analysis (TGA) determines decomposition and mass loss over a temperature range. Differential thermal analysis (DTA) determines endothermic and exothermic event temperatures and shows phase transitions. The TGA/DTA analysis was done by delicately grinding the TU, MgSO₄-doped TU, and metal complexes of MgSO₄-doped TU powdered sample to 0.992 mg placed by the crucible deep Al2O₃ pan for STA2500 to find the thermal stability of the grown crystals of TU, MgSO₄-doped TU, and metal complexes of MgSO₄-doped TU from thermal analysis by NETZSCH STA 2500 at a heating rate of 20°C/min in the temperature range of 30°C to 500°C under the nitrogen atmosphere. The TGA curve observed by the grown TU crystal is shown in Fig. 8 (a) shows the decomposition/mass change over a temperature range of up to 30°C and the mass change of -0.91%. The TGA has observed three stages of decomposition and mass change. The first stage of the decomposition of the temperature was noticed at 30°C to 100°C, and the mass change was -0.91%. The second stage was observed at 30°C to 500°C, with a mass change of -93.76%, and the final stage was observed at 100°C to 500°C, with a mass change of -92.88%. The DTA curve shows that in Fig. 8 (a). It is observed that three fine endothermic peaks are obtained in the grown TU crystal. The starting stage of the endothermic peaks is observed at 180.94°C. The second stage of the endothermic peak of TU observed at 208.44°C. The finishing stage of the endothermic peak of TU was noticed at 458.44°C. This DTA curve shows the TU crystal nature was good, as also determined by the sharpness of the endothermic peaks.

The TGA curve was observed by the grown MgSO₄-doped TU crystal, as shown in Fig. 8 (b), which shows the decomposition and mass change over a temperature range up to 30°C and

the mass change of -2.59%. The TGA has observed three stages of decomposition and mass change. The first stage of the decomposition of the temperature was noticed at 30°C to 100°C, and the mass change was -2.59%. The second stage was observed at 30°C to 495°C and the mass change was -99.91%, and the final stage was observed at 100°C to 495°C and the mass change was -97.32%. The DTA curve shows that in Fig. 8 (b). It is observed that three fine endothermic peaks are obtained in the grown MgSO₄-doped TU crystal. The starting stage of the endothermic peaks is observed at 181.28°C. The second stage of the endothermic peak of MgSO₄-doped TU observed at 203.78°C. The finishing stage of the endothermic peak of MgSO₄-doped TU was noticed at 411.28°C. This DTA curve shows that the MgSO₄-doped TU crystal nature was good, as also determined by the sharpness of the endothermic peaks.

The TGA curve observed by the grown MgSO₄-doped TU metal complexes of crystals shows Fig. 8 (c) has the decomposition/mass change over a temperature range that shows that up to 30°C and the mass change is -99.58%. The TGA has observed only one stage of decomposition and mass change: the stage of decomposition of the temperature was noticed at 30°C to 222°C and the mass change at -99.58%. The DTA curve shows that in Fig. 8 (c). It is observed that three fine endothermic peaks are obtained in the grown MgSO₄-doped TU metal complex crystal. The starting stage of the endothermic peaks is observed at 80°C. The second stage of the endothermic peak of MgSO₄-doped TU metal complexes observed at 182.5°C. The finishing stage of the endothermic peak of MgSO₄-doped TU metal complexes was noticed at 200°C. This DTA curve shows that the MgSO₄-doped TU metal complex crystal nature was good, as also determined by the sharpness of the endothermic peaks.

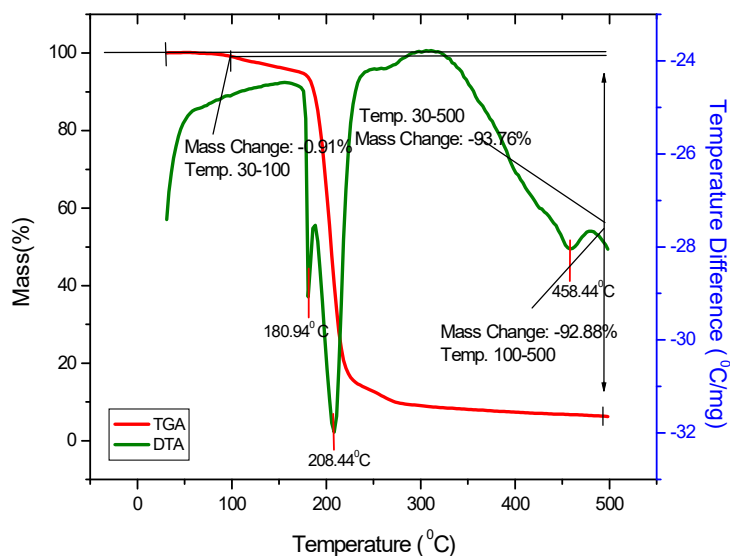


FIG. 8. (a) The TGA/DTA curve of the grown TU crystal.

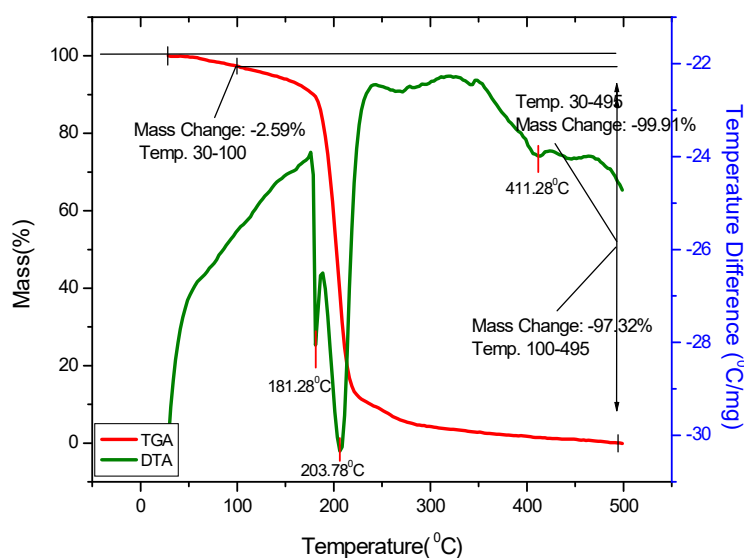


FIG. 8. (b) The TGA/DTA curve of the grown $MgSO_4$ doped TU.

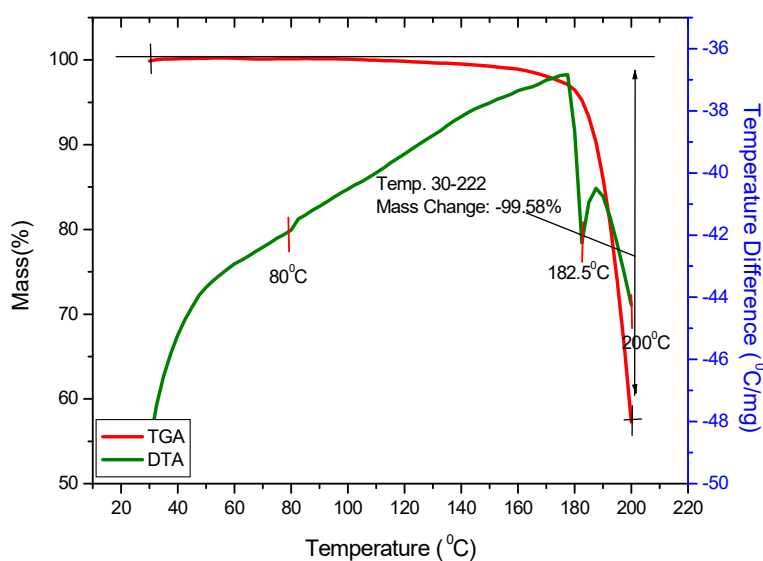


FIG. 8. (c) The TGA/DTA curve of the grown $MgSO_4$ doped TU metal complexes.

Conclusion

Pure and MgSO₄-doped metal complexes of TU could be grown in various dimensions. The change in morphology of the metal complexes of TU was noticed. The unit cell volume of the MgSO₄-doped crystal was slightly decreased. The FTIR spectrum of pure, MgSO₄-doped, and metal complexes of TU shows the incorporation

of the dopants. The EDXA analysis confirms the formation of a metal complex in TU. The UV-visible transmittance shows that the metal complex of TU at the lower cut-off wavelength was found to be enhanced by 14.85nm. The thermal study shows that the metal complex of TU possesses good thermal stability.

References

- [1] Narayan Bhat, M. and Dharma Prakash, S.M., *Journal of Crystal Growth*, 236 (2002) 376.
- [2] Shaked, A., Altaf, A., Qureshi, A.M. and Badshah, A., *J. of Drug Design and Medicinal Chemistry*, 2 (1) (2016) 10.
- [3] El-Bahy, G.M.S., El-Sayed, B.A. and Shabana, A.A., *Vib. Spectrosc.*, 31 (2003) 101.
- [4] Kumari, R.G., Ramakrishnan, V., Carolin, M.L., Kumar, J., Sarua, A. and Kuball, M., *Spectrochimica Acta Part A: Molecular and Bimolecular Spectroscopy*, 73 (2) (2009) 263.
- [5] Fleck, M. and Petrosyan, A.M., *J. Cryst. Growth*, 312 (2010) 2284.
- [6] Puzzarini, C., *The Journal of Physical Chemistry A*, 116 (17) (2012) 4381.
- [7] Anie Roshan, A., Joseph, C. and Ittyachen, M.A., *Mater. Lett.*, 49 (2001) 299.
- [8] Sanwal, K., *Pro. Crystal Growth*, 19 (1989) 189.
- [9] Handricks, S.B., *T. Am. Chem. Soc.*, 50 (1928) 2455.
- [10] Selvakumar, S., Packiam Julius, J., Rajasekar, S.A., Ramanand, A. and Sagayaraj, P., *Mater. Chem. Phys.*, 93 (2005) 356.
- [11] Selvakumar, S., Rajarajan, K., Ravikumar, S.M., Vetha Potheher, I., Prem Anand, D. and Sagayaraj, P., *Cryst. Res. Technol.*, 41 (2006) 766.
- [12] Rajesh, N.P., Kannan, V., Ashok, M., Sivaji, K., Santhana Raaghavan, P. and Ramasamy, P., *J. Cryst. Growth*, 262 (2004) 561.
- [13] Venkataraman, V., Dhanaraj, G., Wadhawan, V.K., Sherwood J.N. and Bhat, H.L., *J. Cryst. Growth*, 154 (1995) 92.
- [14] Ambujam, K., Thomas, P.C., Aruna, S., Prem Anand, D. and Sagayaraj, P., *Cryst. Res. Technol.*, 41 (2006) 1082.
- [15] Sivasankaran, S., Illangovan, S. and Arivoli, S., *International Journal of Engineering Science Invention*, 6 (10) (2017) 05.
- [16] Kannan, B., Seshadri, P.R., Illangovan, K. and Murugakoothan, P., *Indian Journal of Science and Technology*, 6 (7) (2013) 4909.
- [17] Santhi, G. and Alagar, M., *Imperial Journal of Interdisciplinary Research (IJIR)*, 2 (1) (2016) 537.
- [18] Kalaivani, R., Darlin Mary, A., Minisha, S. and Johnson, J., *International Journal of Research and Analytical Reviews (IJRAR)*, 7 (1) (2020) 997.
- [19] Jean Mohan Dass, P.N., Umarani, P.R., Victor Antony Raj, M. and Madhavan, J., *Der. Pharma. Chemica.*, 5 (4) (2013) 262.
- [20] Smith, B.C., "Infrared Spectral Interpretation: A Systematic Approach/ Brain C, Smith". (CRC Press LLC, Boca Raton London New York Washington D.C, 1998) 1-265.
- [21]. Zheng, Z.P. and Fan, W.H., *Journal of Biological Physics*, 38 (3) (2012) 405.